

Developing a Parametric Downconversion  
Apparatus for Single-Photon Experiments in  
Quantum Optics

By

Stephen DiIorio

\* \* \* \* \*

Submitted in partial fulfillment  
of the requirements for  
Honors in the Department of Physics and Astronomy

UNION COLLEGE

June, 2015

## Abstract

DIIORIO, STEPHEN Developing a Parametric Downconversion Apparatus for Single-Photon Experiments in Quantum Optics. Department of Physics and Astronomy, June 2015.

ADVISOR: Orzel, Chad

We report our progress toward developing a parametric downconversion apparatus for studying single-photon quantum optics in undergraduate laboratory classes, following the model of Galvez et al. [1]. We pump a beta barium borate (BBO) crystal with a 405 nm diode laser to produce correlated pairs of single-photons that we detect using avalanche photodiodes (APD). We can conduct coincidence and anticoincidence counts and a measurement of the degree of second-order coherence with the apparatus, and we report a  $g^{(2)} < 1$ . We also discuss the headway towards developing a single-photon interferometer.

# Contents

<b>1</b>	<b>Introduction</b>	<b>1</b>
<b>2</b>	<b>Apparatus</b>	<b>13</b>
<b>3</b>	<b>Measurements</b>	<b>16</b>
<b>4</b>	<b>Results</b>	<b>17</b>
<b>5</b>	<b>Conclusion</b>	<b>20</b>
<b>6</b>	<b>Acknowledgments</b>	<b>21</b>

## List of Figures

1	The Classical HBT Experiment . . . . .	2
2	The Quantum HBT Experiment . . . . .	3
3	Photon Bunching and Antibunching . . . . .	4
4	A More Mathematical Hanbury Brown and Twiss Experiment . . . . .	6
5	Parametric Downconversion . . . . .	10
6	Single-Photon Interferometry . . . . .	12
7	Schematic for Coincidence Counts . . . . .	15
8	Schematic for Anticoincidence Counts and $g^{(2)}(0)$ Measurement . . . . .	16
9	Laser Threshold . . . . .	17
10	Laser Spectrum . . . . .	18
11	Varying Coincidence Counts as a Function of Light Polarization . . . . .	18
12	Varying Anticoincidence Measurements with Polarization . . . . .	20

## List of Tables

1	Pin Layout for Coincidence Counts . . . . .	14
2	Average Coincidence Counts . . . . .	19
3	Average Anticoincidence Counts . . . . .	19

# 1 Introduction

Recent laboratory advancements for performing experiments with single photons allow us to demonstrate the wave-particle duality of light. Kimble et al.'s [2] experiment was the first to experimentally show the existence of nonclassical fields, proving that that can be described as a photon. Since then, advancements in single-photon sources have allowed us to develop more elegant experiments that demonstrate the quantum nature of light and confirms what the photoelectric effect suggested but could not definitively prove.

The photoelectric effect occurs when we produce a current through a piece of metal by shining light onto it. It might be tempting to imagine that this is evidence for the existence of light as a photon, or, more informally, a small particle of energy, that knocks an electron out of the atoms within the metal. This explanation, however, is not entirely accurate and the photoelectric effect can be explained by thinking of the atoms as quantized but the electric fields as not [3]. So this leads us to ask: how do we show the wave-particle duality of light?

The proof of photons' existence begins with astronomers Hanbury Brown and Twiss (HBT) [4]. In an effort to obtain a more accurate way of measuring the size of stellar objects, HBT developed an experiment using a 50/50 silver mirror to look at the correlation between photocurrents of two different detectors. They introduced a time delay in one of the photocurrents to simulate placing these detectors very far from one another, like what they might do in astronomy experiment to highly resolve an image of a star. A diagram of their experiment is shown in Figure 1. They showed that light intensity between two detectors was correlated; if the intensity of one detector went up, then the other detector noticed the same increase. While their experiment did not explore or prove any quantum behavior, it was a historical milestone that got scientists thinking about how to formulate a more complete description of light.

What HBT were really taking note of was a correlation measurement, namely a measurement of the second-order correlation function. First we approach this from a classical setting, where Maxwell's equations can fully describe light. We can define the correlation between the transmitted and reflected intensities of a beam,  $I_T$  and  $I_R$  respectively, with a function that relates a time delay,  $\tau$ , with the intensity of incoming light onto the detectors

$$g_{T,R}^{(2)}(\tau) = \frac{\langle I_R(t)I_T(t + \tau) \rangle}{\langle I_R(t) \rangle \langle I_T(t + \tau) \rangle}, \quad (1.1)$$

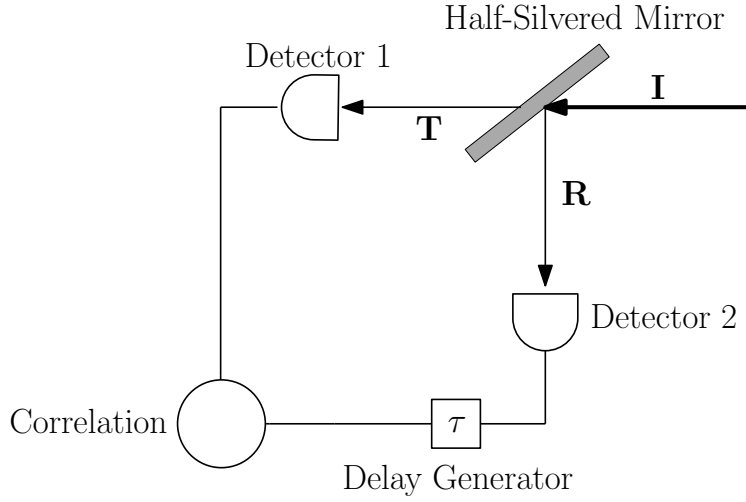


Figure 1: Here we show incident light,  $I$ , on a half-silvered mirror. In the experiment that HBT conducted, they saw that the photocurrents produced by each of the detectors caused by the reflected,  $R$ , and transmitted,  $T$ , light was correlated as they changed the time delay,  $\tau$ .

where  $\langle \dots \rangle$  indicates a timed average.

The conflict arose when the results of this experiment were approached in two different contexts: considering light as a wave and considering light as a particle. When light is thought of classically, as a wave, and we consider simultaneous intensity measurements ( $\tau = 0$ ) of the incident, reflective, and transmitted light that passes through a 50/50 beam splitter, it is very probable to notice simultaneous detection of light hitting either detector at the same time. It follows that (1.1) becomes

$$g_{T,R}^{(2)}(0) = g_{I,I}^{(2)}(0) = g^{(2)}(0) = \frac{\langle [I_I(t)]^2 \rangle}{\langle I_I(t) \rangle^2}, \quad (1.2)$$

and it follows that (1.2) has values  $\geq 1$ , as HBT observed.

A measurement like this, however seemed to be impossible when considering light as a photon. In the same situation, where a single photon is incident on a beam splitter, it can either transmit or reflect through the beam splitter, but it cannot do both. As such, we would see a hit at only one of the detectors (there would be no coincidences) and would find  $g^{(2)} = 0$  when  $\tau = 0$ . Thus, the goal of future experiments was to prove that light could exist in single states.

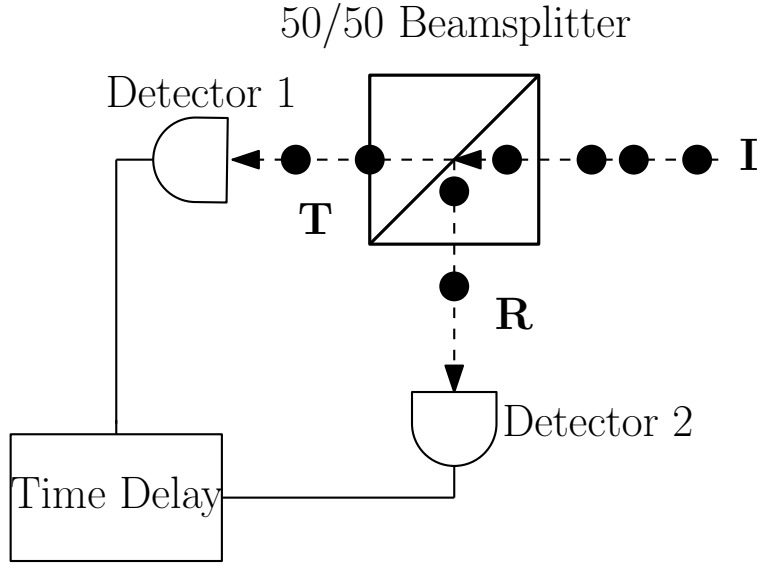


Figure 2: In this setting, we send photons through a beam splitter that either reflect or transmit to hit single-photon detectors. These detectors send a signal to a counter that measures the time delay between received signals at Detector 1 and Detector 2 and the number of counts each detector received.

In an effort to explain this, we can look at the HBT experiment from a quantum perspective. In this experiment, instead of looking at a continuous wave incident on a beam splitter, we have a stream of photons entering the system. As described before, the photons either reflect off the beam splitter or transmit through it. These photons are now incident on single-photon detectors and we measure the time difference between signals received from Detector 1 and Detector 2; we also count the number of photons received at each detector. Figure 2 shows a schematic of the experiment.

In this setting,  $\tau$  measures the time delay between incoming signals from either detector. Knowing that the number of photons we receive at either detector is a function of the intensity of light, we can rewrite (1.1) as

$$g^{(2)}(\tau) = \frac{\langle n_1(t)n_2(t + \tau) \rangle}{\langle n_1(t) \rangle \langle n_2(t + \tau) \rangle}, \quad (1.3)$$

where  $n_1(t)$  is the number of counts Detector 1 receives and  $n_2(t)$  is the number of counts Detector 2 receives. What is important to note here is that the value of  $g^{(2)}(\tau)$  is proportional to the probability of receiving a count at some time  $t = \tau$  given we received a count at time  $t = 0$ .



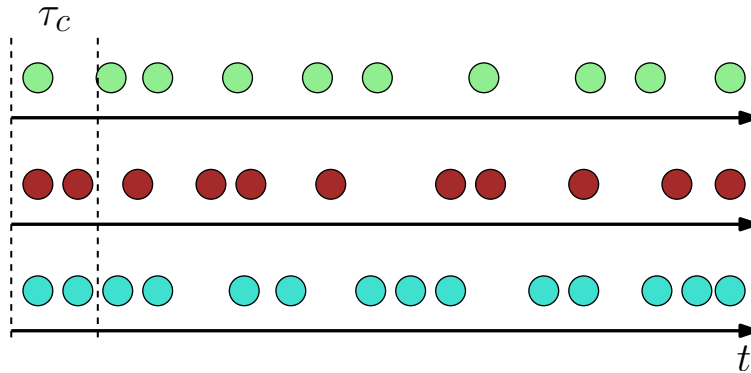


Figure 3: When describing how light bunches, we ideally look at a small time interval or the coherent time of the light source,  $\tau_c$ , and observe how many photons pass by. The top row shows antibunching light, where there is a large time delay between receiving incoming photons. The middle row shows random or coherent light, where we sometimes only see one photon pass by and sometimes we see a group of them pass by. The bottom row is bunched or chaotic light, where we see large groupings of photons pass by in a given time interval.

Given this, we can then consider three different circumstances describing the stream of photons through a system, and Figure 3 shows the three different circumstances that can arise. In the first case we can imagine a consistent stream of photons that are all grouped together in bunches. In a setting such as this, it is easy to imagine several photons incident on a beam splitter and there being a high probability of detecting signals from both detectors within a very short period of time. Thus,  $g^{(2)}(\tau)$  is a large number for small values of  $\tau$ . We would get a measurement of  $g^{(2)}(\tau) > 1$ . Bunched light is usually produced by a thermal source.

In the extreme opposite, we could have a light source that is not bunched at all, but provides individual photons at regular intervals. This is referred to as antibunched light. In this case, the time separation between subsequent photons is so large that there is a very low probability of receiving a signal from both detectors for small values of  $\tau$ . Thus, we would get a measurement of  $g^{(2)}(\tau) < 1$ . Antibunched light is produced by single photon sources.

In another setting, which is a combination of the two, we have a stream of photons that is coherent, or random. Here we might find single photons enter our system or we might find bunches of photons entering. With these random time intervals between receiving incoming photons, it is just as likely that we may detect two photons within a short time period of one another as it is that we have to wait a long

time before detecting a second photon. In other words, the values of  $g^{(2)}(\tau)$  that we measure between subsequent detections averages out to a value of 1, since the the probability of receiving a second signal after some initial photon enters the system is the same for all  $\tau$ . Coherent light is usually produced by with laser light.

An important note here is that random and bunched light can be explained by the classical, wave-like behavior of light that we most commonly notice. Antibunched light, however, fails to satisfy our classical description of light and can only be explained as a quantum effect; there is no classical description that correlates with this behavior of light. Thus, if we can experimentally show  $g^{(2)}(0) < 1$ , which can only happen with antibunched light, we can show light's particle behavior and explore the wave-particle duality of light.

Having explained both the classical and quantum results we can expect when we think of the HBT experiment in two different lights, it is useful to show how we mathematically achieve  $g^{(2)}(0) = 0$  given a single-photon Fock state. Figure 4 shows the HBT experiment in this context. The system is set up to count coincidences that occur when Detector 3 receives a hit at time  $t$  and when Detector 4 receives a hit at time  $t + \tau$ . We can then write the second-order correlation function as

$$g^{(2)}(\tau) = \frac{\langle n_3(t)n_4(t + \tau) \rangle}{\langle n_3(t) \rangle \langle n_4(t + \tau) \rangle}, \quad (1.4)$$

where, again,  $n_3(t)$  and  $n_4(t)$  are the number of photons Detectors 3 and 4 receive at time  $t$ , respectively.

Given that the photon number operator,  $\hat{n} = \hat{a}^\dagger \hat{a}$ , where  $\hat{a}^\dagger$  is the creation operator and  $\hat{a}$  is the annihilation operator, at time  $t = 0$  we can write Equation (1.4) as

$$g^{(2)}(0) = \frac{\langle \hat{a}_3^\dagger \hat{a}_4^\dagger \hat{a}_4 \hat{a}_3 \rangle}{\langle \hat{a}_3^\dagger \hat{a}_3 \rangle \langle \hat{a}_4^\dagger \hat{a}_4 \rangle}. \quad (1.5)$$

In order to evaluate  $g^{(2)}(0)$  for an arbitrary state, we first relate the creation and annihilation operators of the output fields to the input fields of the beam splitter. For the classical fields, we can write

$$\mathcal{E}_3 = (\mathcal{E}_1 - \mathcal{E}_2)/\sqrt{2}, \quad (1.6)$$

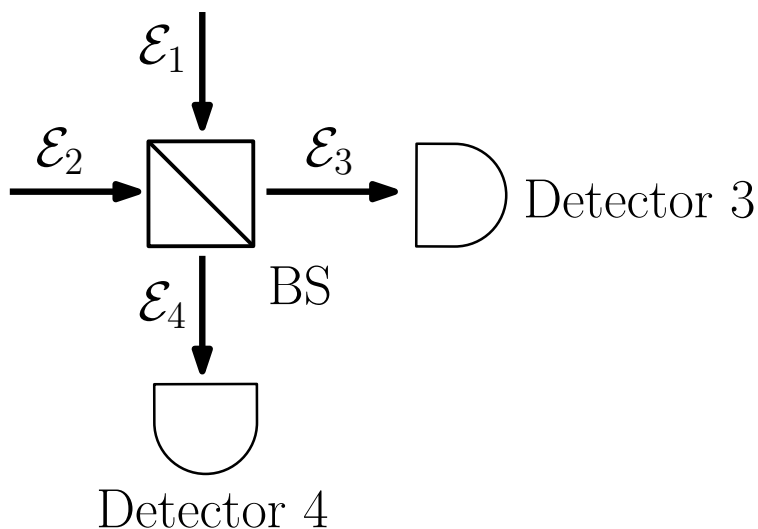


Figure 4: Here, we look again at the HBT experiment. The four ports into and out of the beam splitter are labeled with the subscripts, and  $\mathcal{E}_i$  refers to the electric field at port  $i$ . Detectors 3 and 4 are set to detect output fields  $\mathcal{E}_3$  and  $\mathcal{E}_4$ . We investigate the system when light enters port 1.

$$\mathcal{E}_4 = (\mathcal{E}_1 + \mathcal{E}_2)/\sqrt{2}. \quad (1.7)$$

We can apply the same relationships to the annihilation operators for the output fields:

$$\hat{a}_3 = (\hat{a}_1 - \hat{a}_2)/\sqrt{2}, \quad (1.8)$$

$$\hat{a}_4 = (\hat{a}_1 + \hat{a}_2)/\sqrt{2}, \quad (1.9)$$

where the  $\frac{1}{\sqrt{2}}$  comes from the 50/50 power splitting from the beam splitter, and the minus and plus signs in either equation come from a phase shift from reflections in the beam splitter.

In this experiment, light was only introduced in port one of the beam splitter, meaning the field at port two the vacuum. This allows us to write the input states as

$$|\Psi\rangle = |\psi_1, 0_2\rangle \quad (1.10)$$

where  $|\psi_1\rangle$  is an arbitrary state at port one, and  $|0_2\rangle$  is the vacuum state at port two. With this, we can derive

$$\langle \hat{a}_3^\dagger \hat{a}_3 \rangle = \langle \psi_1 | \hat{n}_1 | \psi_1 \rangle / 2 \quad (1.11)$$

using Equation (1.8) and

$$\langle \hat{a}_4^\dagger \hat{a}_4 \rangle = \langle \psi_1 | \hat{n}_1 | \psi_1 \rangle / 2 \quad (1.12)$$

using Equation (1.9). We can also derive, using the same equations,

$$\langle \hat{a}_3^\dagger \hat{a}_4^\dagger \hat{a}_4 \hat{a}_3 \rangle = \langle \psi_1 | \hat{a}_1^\dagger \hat{a}_1^\dagger \hat{a}_1 \hat{a}_1 | \psi_1 \rangle. \quad (1.13)$$

This can be simplified further given the commutation relation  $[\hat{a}, \hat{a}^\dagger] = \hat{a}\hat{a}^\dagger - \hat{a}^\dagger\hat{a} = 1$ , resulting in

$$\hat{a}_1^\dagger \hat{a}_1^\dagger \hat{a}_1 \hat{a}_1 = \hat{n}_1(\hat{n}_1 - 1). \quad (1.14)$$

Using Equations (1.11), (1.12), (1.13), we find

$$g^{(2)}(0) = \frac{\langle \psi_1 | \hat{n}_1(\hat{n}_1 - 1) | \psi_1 \rangle}{(\langle \psi_1 | \hat{n}_1 | \psi_1 \rangle / 2)^2}, \quad (1.15)$$

which leads to

$$g^{(2)}(0) = \frac{\langle \hat{n}(\hat{n} - 1) \rangle}{\langle \hat{n} \rangle^2}. \quad (1.16)$$

For an arbitrary photon number state, this can be written as

$$g^{(2)}(0) = \frac{n(n-1)}{n^2}. \quad (1.17)$$

Thus, for a single-photon Fock state, with  $n = 1$ , we see that  $g^{(2)}(0) = 0$ , and such states have been produced in labs to measure  $g^{(2)}(0)$  values close to zero.

Kimble et al. [2] was the first to experimentally record measurements of  $g^{(2)}(0) < 1$ , suggesting the existence of photons. They were able to observe antibunching by looking at a single atom and its excitement

and then decay. They had a stream of sodium atoms pass in front of a high power laser, such that, on average, there was only one or two atoms excited at a time. These atoms would be excited for a lifetime of  $\tau_r$ , then decay from  $3^2P_{3/2} \rightarrow 3^2S_{1/2}$  and emit 589 nm light. Because they used a high power laser, the sodium atoms would quickly excite again such that the time span between decay and excitation becomes negligible, so the timing between photons effectively becomes  $\tau_r$ . This light was sent to a 50/50 beam splitter, and the reflected and transmitted beams were sent to photomultipliers to record the coincidences. They were unable to find a  $g^{(2)}(0) = 0$ , like they predicted, but instead found  $g^{(2)}(0) = 0.4$ . Still, this result suggested that the field was antibunched, where photons arrived at the detectors at regular intervals.

The problem with this experiment was twofold: their laser light and fluorescent light were at the same frequency and it was not always the case that they had a single excited atom in the system at a time. Because they couldn't isolate just the fluorescence, the detectors picked up stray light and produced accidental coincidences. And because there was the possibility for more than one sodium atom to be excited at a time, there was the chance that more than one photon was emitted at a time, also creating accidental coincidences.

Grangier et al. [5] performed a similar experiment, but got a value of  $g^{(2)}(0) = 0.18 \pm 0.06$ . They got around unwanted background light triggering events by using calcium atoms as their source. They too had a stream of calcium atoms flow past a laser composed of frequencies  $\nu_{I1}$  and  $\nu_{I2}$ . This beam caused the calcium to undergo two-photon excitation from  $4'S_0$  to  $6'S_0$ . It decays to a short lived energy level, emitting a 551 nm (green) light,  $\nu_1$ , and then quickly decays again to the ground state, emitting 423 nm (blue) light,  $\nu_2$ . Since they had two different frequencies of light, it was easy to filter and control the light detected in their experiment. To conserve angular momentum, when the calcium atom decays, the two photons are emitted in opposite directions. Because of this, they placed one detector to act as a gate so that they knew when to expect a single photon at their beamsplitter. In this experiment, the green light activated the gate and was used to measure the arrival of the blue light. From this, we can also determine the second order of coherence based on the probability of measuring coincidences at the gate, reflected, or transmitted detectors, and it becomes

$$g^{(2)}(0) = \frac{P_{GTR}}{P_{GT}P_{GR}} = \frac{N_{GTR}N_G}{N_{GT}N_{GR}} \quad (1.18)$$

where  $P$  is the probability of finding simultaneous photocounts and  $N$  is the number of single counts, both

at the respective detectors. The measurement Grangier et al. made was definitely evidence for the existence of photons, and they only measured 9 out of the 50 threefold coincidences (when all three detectors were triggered at the same time) expected from a classical explanation.

While Grangier et al.'s results were more convincing of the notion that photons existed, Thorn et al. [6] performed a similar experiment that got better results faster and more effectively. Thorn et al. created a method for detecting photons using parametric downconversion. With this, they were able to use a gate system, like Grangier et al. Thorn et al. took advantage of technology that wasn't available in Grangier et al.'s time and, within a five minute experiment, measured a  $g^{(2)}(0) = 0.0188 \pm 0.0067$ , and the nonzero result can be fully explained from the accidental coincidences.

Instead of using calcium to create two photons, Thorn et al. used a parametric downconversion source. In previous methods mentioned, experimenters would have to isolate and trap atoms to perform experiments on, a difficult challenge in its own right, and these atoms could deexcite and emit a photon in a any direction, decreasing the efficiency of measurements in an experiment. Parametric downconversion is a more efficient method for its simplicity, reduced cost, and increased count rates. Parametric downconversion is the process of converting a photon of one frequency to two separate photons, each with a frequency half the original photon. The only downside to using parametric downconversion is that the power output is much less than the input and these beams have to be detected using photon counting. Despite this, downconversion is still a more efficient method than exciting calcium atoms.

These resulting conversions still obey the laws of conservation of energy such that the pump,  $p$ , (our laser input) and the signal,  $s$ , and idler,  $i$ , (the two downconverted photons) obey

$$E_p = E_s + E_i, \hbar\omega_p = \hbar\omega_s + \hbar\omega_i, \omega_p = \omega_s + \omega_i. \quad (1.19)$$

They also obey conservation of momentum such that

$$\vec{k}_p = \vec{k}_s + \vec{k}_i \quad (1.20)$$

where  $\vec{k}$  describes the wave vector of the field. In this case, there is a Type-I downconversion, where

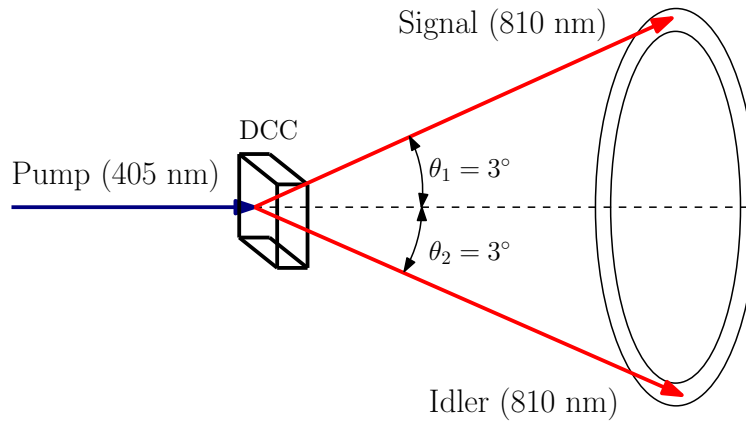


Figure 5: In parametric downconversion, we pump a non-linear, downconversion crystal (DCC) with laser light, in this case 405 nm light. This undergoes a non-linear process in which the blue light is absorbed and converted into two separate photons of half the energy of the original. To conserve angular momentum, these two photons also come out at known angles with respect to the optical axis. The possible locations either photon will strike forms a ring, which makes placing detectors to pick up the photons much easier to do and greatly increases the efficiency of our experiments.

the polarizations of the two exiting photons are parallel to each other but perpendicular to the pump's polarization. The crystal is designed so the signal and idler photons separate from each other and the pump beam over some distance. Figure 5 schematically shows what happens with parametric downconversion.

Using parametric downconversion to produce single photons to make a measurement of  $g^{(2)}(0)$ , Thorn et al. aimed a 409 nm (UV) diode-pumped, frequency-doubled, solid-state laser at a nonlinear beta-borium borate crystal. Before it reached the crystal, the pump passed through a 400 nm half-wave plate, that adjusted the polarization of the beam to maximize the chance of downconversion. This crystal was designed to convert 405 nm light into 810 nm signal and idler beams that branched out  $3^\circ$  from the pump beam. Only some of the photons undergo this transition. After this conversion, the two IR beams leave the crystal. The idler is aimed directly at the gate photodetector, G, which serves a similar purpose as the gate detector in the Grangier et al. experiment, and the signal beam is aimed at a half-wave plate that polarizes it  $45^\circ$  with respect to the polarization axis of the polarizing beamsplitter. This allows for the light to split equally into the the T and R detectors. A detection at the G detector indicates to the system that the experiment is taking place and to expect a single photon to come through and hit either the R or T detector. These measurements at the R and T detectors are used to determine the second-order coherence.

Using this process, Thorn et al. took about 100 measurements of  $g^{(2)}(0)$  and varied the length of each experiment. After five minutes, they found that  $g^{(2)}(0) = 0.0188 \pm 0.0067$  and after a separate experiment that lasted forty minutes, they found  $g^{(2)}(0) = 0.0177 \pm 0.0026$ , which was their best result. The reason they did not get an exact result of  $g^{(2)}(0) = 0$  was because of the possibility that other photons created from different downconversion events struck either T or R. Their results, when they accounted for these accidental coincidences, became  $g^{(2)}(0) = 0.0164$ , which is within their statistical error.

Thorn et al. provides evidence to suggest that light behaves in a way that only quantum mechanics can describe. They created an efficient method designed for undergraduates, so that they could observe quantum mechanical events. Their design was costly, but its parts were readily available and flexible enough to be used in several other experiments. The experiment itself was designed to be simple to construct and provided accurate results in a short period of time; a five minute experiment produced a result an order of magnitude more accurate than what Grangier et al. could produce, and their most accurate result only took forty minutes. Not only this, their errors can be explained when we consider accidental coincidences that might occur during the experiment.

We build off the same experimental set up that Thorn et al. designed and follow a similar procedure to Galvez et al. [1] in producing a series of experiments for undergraduates to explore the wave-particle duality of light. There has been work over the years to perfect and improve upon the efficiency and breadth of the experiments we are capable of performing using this experimental set up [7, 8, 9, 10].

We perform three different experiments and report on the construction of a fourth. We perform coincidence counts, anticoincidence counts, a measurement of  $g^{(2)}(0)$ , and report on the construction of a single-photon interferometer. The coincidence counts experiment is a proof-of-concept where we show that our apparatus indeed produces single photons that we can detect. The beauty of starting with this experiment is that we develop a system that is modular. All of the subsequent experiments are based on the same premise and components used in this experiment. The idler photon is used to start any measurements and the signal photon goes through a separate experimental set up before reaching a detector.

The anticoincidence count experiment is a similar set up to the experiment Thorn et al. conducted and allows us to show the particle behavior of light where we can only receive coincidence counts between the



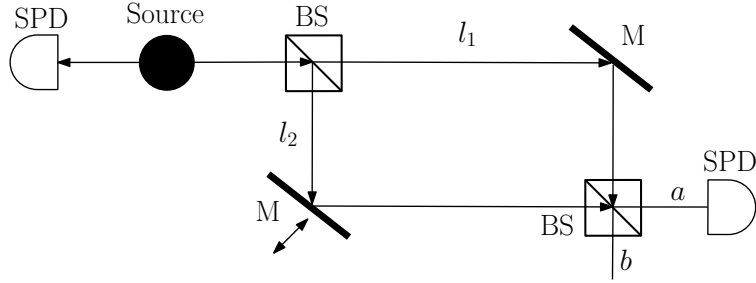


Figure 6: Here we show a schematic of the single-photon interferometer set up. The source produces the single photons that get sent to the gate detector (an SPD, single photon detector) and the Mach-Zehnder interferometer. The photon in the interferometer can travel down the arm of length  $l_1$  or of length  $l_2$ . To alter the length of one of the arms, and thus cause an interference pattern, the position of one of the mirrors is adjustable with a piezoelectric. The photon, after traveling through one of these paths, can exit the second beam splitter shown at either port  $a$  or port  $b$ .

gate and either the reflected or the transmitted detector. We can also change the polarization of the light to switch which detector receives a signal. A  $g^{(2)}(0)$  measurement can be made with the same set up as Thorn et al. used.

Finally, we report on the progress in the construction of a single-photon interferometer. In this experimental set up, we still use the idler photon to act as a trigger to start taking a measurement. The heart of the experiment, however, is making a single photon interfere with itself using a Mach-Zehnder interferometer. Figure 6 shows a schematic of the interferometer in question. As a photon enters the first beam splitter of the interferometer, there are two possible outcomes: either it transmits through and has an amplitude of  $t$  or it reflects off the splitter and has an amplitude of  $r$ . Once the photon leaves the beam splitter, however, the photon is in a superposition of having traveled down both arms of the interferometer. This can be expressed as

$$|s\rangle = t|l_1\rangle + r|l_2\rangle, \quad (1.21)$$

where  $|s\rangle$  refers to the state of the photon and  $|l_1\rangle$  and  $|l_2\rangle$  refer to the state of the photon in either arm of the interferometer. We can write  $|l_1\rangle$  and  $|l_2\rangle$  as

$$|l_1\rangle = e^{i\delta_1}(r|a\rangle + t|b\rangle), \quad (1.22)$$

$$|l_2\rangle = e^{i\delta_2}(t|a\rangle + r|b\rangle), \quad (1.23)$$

where  $\delta_i = kl_i$ , where  $k$  is the wavenumber of the photon in question and  $l_i$  is the length of arm  $i$ , and  $|a\rangle$  and  $|b\rangle$  refer to the state of the photon as it leaves either the  $a$  or  $b$  port of the interferometer, respectively. Thus, we can write the probability of finding the photon leaving the  $a$  port as

$$P(\delta) = |\langle a|s\rangle|^2 = 2RT(1 + \cos(\delta)), \quad (1.24)$$

where  $R$  and  $T$  are the reflection and transmission probabilities, respectively. A similar argument can be made for the probability of finding a photon leave port  $b$ . What we find is that the probability of detecting a photon leaving either port is a function of the path length through which it travels, which, in our case, is a function of the voltage applied to the piezoelectric.

The rest of this document is to serve as a description of the particular nuances that goes into the construction of these experiments.

## 2 Apparatus

Here, we will discuss the different components necessary to conduct coincidence counts, anticoincidence counts, and single-photon interferometry experiments. Firstly, we discuss the equipment that is consistent and essential for all three (and all future) experiments. A Helium-Neon (HeNe) laser is used for alignment purposes, and optics are arranged to direct this laser light to follow the same paths we would expect the downconverted photons to follow. To perform the experiments we use a 405 nm GaN diode laser, powered by a Thorlabs LDC205C current supply and temperature controlled by a Thorlabs TED200C temperature controller.

We use Excelitas SPCM-EDU CD3375H avalanche photodiodes (APD) to detect single photon counts. These output a 5.5 V signal with a 50  $\Omega$  impedance when they received a ‘‘hit.’’ The detectors themselves are powered by their own power supplies that provided 5 V voltage. To process the signals produced by the APDs, an adapter box is used and allows for four APDs to communicate with it simultaneously via BNC cables. These four ports are labeled  $A$ ,  $A'$ ,  $B$ , and  $B'$ . An Altera DE2 circuit board interfaces with this

Switch 1	Switch 2	Switch 3	Switch 4	Coincidence Recording
<i>A</i>	<i>B</i>	<i>A'</i>	<i>B'</i>	
0	0	0	0	None
0	0	0	1	<i>B'</i>
0	0	1	0	<i>A'</i>
0	0	1	1	<i>A' B'</i>
0	1	0	0	<i>B</i>
0	1	0	1	<i>B B'</i>
0	1	1	0	<i>B A'</i>
0	1	1	1	<i>B A' B'</i>
1	0	0	0	<i>A</i>
1	0	0	1	<i>A B'</i>
1	0	1	0	<i>A A'</i>
1	0	1	1	<i>A A' B'</i>
1	1	0	0	<i>A B</i>
1	1	0	1	<i>A B B'</i>
1	1	1	0	<i>A B A'</i>
1	1	1	1	<i>A B A' B'</i>

Table 1: This table corresponds to the different pin configurations that lead to different coincidence counts, where 0 means the switch is off and 1 means the switch is on. These switches on the board itself are in groups of four. Switch 1 starts on the right, and we progress to the left to change subsequent switches. When multiple switches are on, then we record the coincidence counts between those detectors. In other words, we only consider there to be an actual count when all of the detectors receive a “hit” within a specific period of time.

adapter box to process the incoming signal. The board is itself programmable in which detectors we can measure counts from. At the bottom of the board are several switches organized in groups of four. Each set of four switches controls which detectors we are interested in recording coincidence counts between. Reading from right to left, the switches control measurements taken from detector *A*, *B*, *A'*, and *B'*. When a switch is on, measurements for that detector are recorded. For example, if just the first switch is on, then we record the counts detector *A* receives, and if both switches 1 and 3 are on, then we record the number of counts detectors *A* and *A'* receive at the same time. Table 1 shows all the possible combinations of these switches and the coincidence recordings they correspond to. The two leftmost switches control the coincidence time resolution.

All of the data collection was done using a LabVIEW program developed at Colgate University. The program used for all of the experiments was named “Coincidence\_rs232(4\_3).vi”.

A Thorlabs WPH10M-405 405 nm half-wave plate was placed in front of the beta barium Borate down-

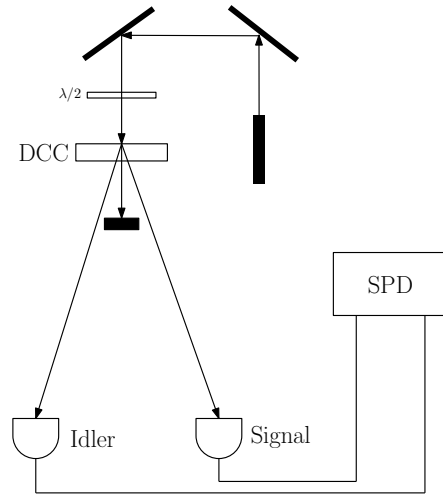


Figure 7: Here is the arrangement of the key components that go into achieving coincidence counts. A 405 nm laser is directed first through a half-wave plate, then through a DCC. The downconverted photons leave at a known angle, and the signal and idler collimators are placed to pick up those photons. The majority of the laser light simply passes through the crystal and is blocked by a beam blocker. The collimators are connected to fiber optics that direct the single photons to the single-photon detectors.

conversion crystal (DCC) in order to maximize the number of downconverted photons we produced. Additionally, all of the experiments used Thorlabs FB810-10 810 nm bandpass filters to prevent as much stray light from entering the system as possible. The filters were placed in front of Thorlabs F220FC-780 780 nm fiber collimators which sent the photons, via fiber optics, to the APDs. No additional equipment was necessary to complete the coincidence counts experiments. Figure 7 shows a schematic of where to place all of the components to complete the coincidence count experiments.

To record anticoincidence counts and to make a measurement of  $g^{(2)}(0)$ , three collimators were used. The idler photon still went to a gate detector to tell the system to start making measurements. The signal photon was sent through a Thorlabs WPH10M-808 808 nm half-wave plate placed in front of a Thorlabs PBS252 polarizing beam splitter. This directed the photon to either the reflected or transmitted collimator to be detected. Figure 8 shows the set up and placement of components to record anticoincidence counts.

For single-photon interferometry, the signal photon was sent to a Mach-Zehnder interferometer. This consisted of two Thorlabs BS005 beam splitters with one of the mirrors placed on a translation stage that could be moved via a piezoelectric attached to its own power supply. Figure 6 shows the layout of all the

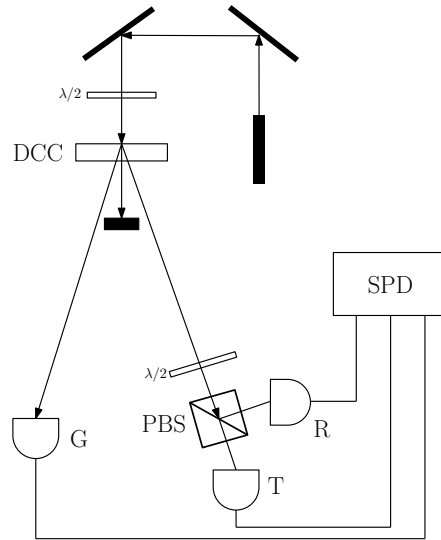


Figure 8: We use the same equipment to record coincidence counts with the addition of several optic pieces that manipulate the signal photon. Here, we use a half-wave plate and a polarizing beam splitter to control whether the photon reflects or transmits through the beam splitter.

components.

### 3 Measurements

All of the measurements were taken with the diode laser at a temperature of 10.024 kΩ, roughly 25°C and supplied with a current of 120 mA. Figure 9 shows the power output of the diode at various currents, and Figure 10 shows the output wavelengths of the diode at this temperature. The number of downconverted photons generated varied as a function of the polarization of the light incident on the crystal. Figure 11 shows how the polarization affects the number of photons we can generate (and, subsequently, affects how many coincidence counts we can detect). For all of the experiments, the half-wave plate was set to polarize the laser light to 243°. Additionally, the APDs were covered with a cloth during the experiments to reduce any change of stray light hitting the detectors. Within the software itself, an update period of 1.0 s was used to capture data.

For the coincidence counts experiment, once all the optics was aligned to achieve the maximum number

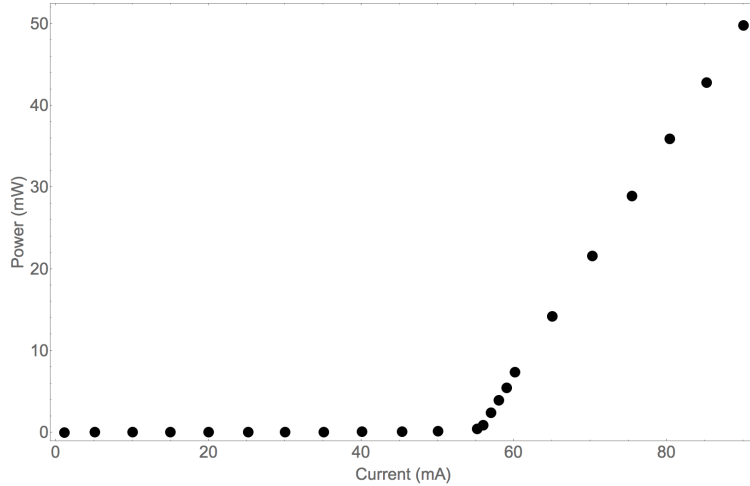


Figure 9: Shown is the power output of the diode used as a function of supplied current. The threshold current is around 55 mA, and the power output increases linearly for larger currents.

of counts, a 5 minute trial was run to see the average number of coincidence counts per second we could receive. Ports  $A$  and  $B$  were used, and the number of hits both detectors received within a window of  $7.39 \pm 0.03$  ns were considered to be real data points.

For the anticoincidence counts experiments, we varied the polarization angle of the half-wave plate in front of the polarizing beam splitter and took measurements at several angles that lasted for 10 s each. The angle of this half-wave plate was  $69^\circ$  so that there was an equal flow of photons headed towards the reflected and transmitted detectors for the  $g^{(2)}(0)$  measurement. The  $g^{(2)}(0)$  measurement was taken over the course of 5 minutes. For both of these experiments, ports  $A$ ,  $B$ , and  $B'$  were used, and the window which all three detectors had to receive a hit in order for there to be a three-fold coincidence count between detectors  $ABB'$  was 4.76 ns.

## 4 Results

The coincidence count experiment was vital in the success of the remainder of the experiments, and ensuring that we received as many coincidence counts as possible increased the efficiency of subsequent experiments. The purpose of this experiment was to demonstrate that our system can record counts that happen

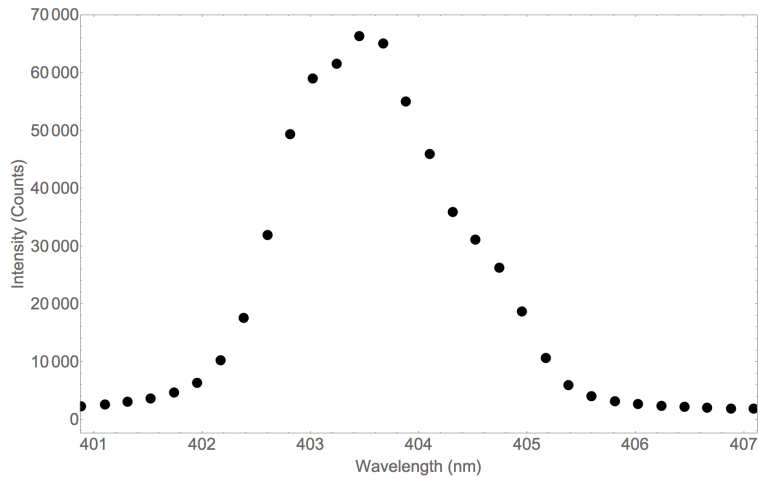


Figure 10: Shown is the spectrum of the diode laser used in the experiments. This particular spectrum was taken when the temperature of the diode was at 25°C. At this temperature, the laser is in single-mode and its output wavelength is centered around 403.5 nm. This measurement was taken using a USB4000 Ocean Optics spectrometer.

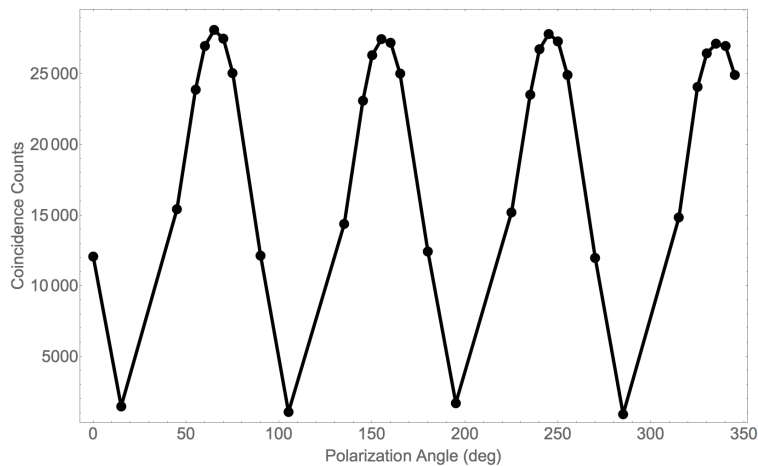


Figure 11: We used the coincidence counts experiment to observe how changing the polarization of the laser light affected the number of downconverted photons generated and, subsequently, how this affected the number of coincidence counts we detected. Unsurprisingly, the number of counts we detected sinusoidally oscillated with a period of 90°.

Port	Counts (cps)
<i>A</i>	349122.3
<i>B</i>	291192.3
<i>AB</i>	25282.3

Table 2: Here we list the average number of counts per second (cps) detectors *A* and *B* received and show how many of those appeared within a finite window.

at two detectors within a certain period of time. Depending on how well the system is set up, we manage to see between 20,000 and 60,000 coincidence counts. Table 2 shows the average number of coincidence counts we could receive between two detectors.

For our anticoincidence counts experiments, the goal was to show that we could switch which two detectors record coincidence counts. Either the gate and the reflected detectors or the gate and the transmitted detectors should record coincidence counts, but we should not notice any coincidence counts between all three detectors. This is unusual, because in a classical understanding of light we would expect light to be able to travel down to both the transmitted and reflected detectors after going through a beam splitter. This, however, is not the case. In Table 3 we show the average number of counts received by each detector. Here, we notice coincidence counts between detectors *AB* and *AB'*. We do not, however, notice any counts between all three detectors except for a few occasional hits. In addition to this, we can change the polarization of the half-wave plate in front of the polarized beam splitter to control which detectors receive coincidence counts. Figure 12 shows how we can change which detectors receive coincidence counts by altering the polarization of the wave plate.

Port	Counts (cps)
<i>A</i>	252476.3
<i>B</i>	138339.2
<i>B'</i>	143580.1
<i>AB</i>	7470.373
<i>AB'</i>	11859.49
<i>ABB'</i>	0.026667

Table 3: Here we list the average number of counts per second (cps) detectors *A*, *B*, and *B'* received. In addition to that, we show how many coincidence counts we detect between various detectors. An important result is that we only notice coincidence counts between *AB* and *AB'*, while there are practically none between all three.



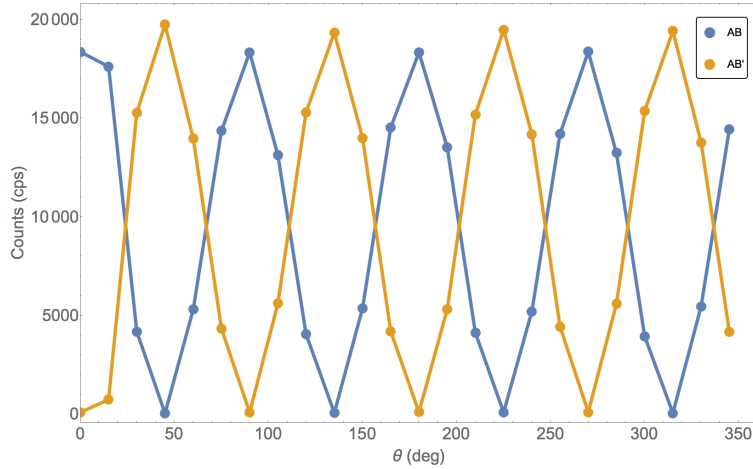


Figure 12: As we change the polarization of the half-wave plate in front of the polarized beam splitter, we control whether or not light transmits or reflects off the beam splitter.

In addition to these measurements, we can also use this set up to make a measurement of  $g^{(2)}(0)$ . With this, we measure  $g^{(2)}(0) = 0.0001 \pm 0.0005$ . This measurement is calculated using the average counts at the respective detectors as follows

$$g^{(2)}(0) = \frac{(A)(ABB')}{(AB)(AB')}. \quad (4.1)$$

The error of this measurement is the standard deviation of all the measurements taken over the course of the experiment.

## 5 Conclusion

Providing experimental evidence for the wave-particle duality of light has become easier over the decades. While experiments have been done in the past to show that light behaves like a particle using trapped atoms, these are more often than not inefficient and complex set ups. With the introduction of parametric downconversion to produce pairs of single photons, the experimental set ups involved in making measurements that show light behaves like a particle have become cheaper and simpler to put together. In addition to that, using downconverted photons allows us to complete quantum optics experiments and record data

within a matter of minutes. This simplicity is ideal in an undergraduate setting as it gives students an easy and digestible means of exploring the properties of light.

Here, we have successfully shown several accessible experiments that demonstrate to undergraduate students the wave-particle duality of light. We first showed that we generate photons from our down-conversion crystal via coincidence counts. This then progressed into showing that light indeed displays particle characteristics with anticoincidence counts. In this setting, we showed that when we introduce a beam splitter into the system, we can measure coincidence counts between the idler detector and either the reflected or the transmitted detectors, but not all three. Additionally, we showed that we can control which detector we can detect all of the coincidence counts at by adjusting the polarization of the produced photons. Finally, we did not manage to completely implement the single-photon interferometer, but we did manage to notice interference patterns with the HeNe laser. Though this is not indicative of a well-aligned system that would allow 810 nm light to interfere with itself, it does show that we are headed in the right direction.

With all of these experiments, we managed to produce a measurement of  $g^{(2)}(0) < 1$ , implying that light does behave as a photon. While this measurement is indicative of the particle behavior of light, it seems too accurate of a measurement given the experimental set up. Errors that could have artificially lowered this value could range from misaligned optics, the blocking of photons that should have been counted, to problems with the experimental set up itself and how we were interacting with the software that calculated the value.

Still, we present the theory explaining how light can behave as both a wave and a particle and provide several experiments that allow students to explore this themselves.

## 6 Acknowledgments

I firstly thank my advisor, Professor Chad Orzel of the Physics and Astronomy Department at Union College, for all he has done for me in my four years here. Secondly, I thank Professor Seyfollah Maleki for his help with progressing this project. Thirdly, I thank the multitude of professors of the physics department, the administrative assistant, Lynnette Stec, and the technician, John Sheehan for making my time here en-

joyable. They are like a second family to me, and I always enjoyed seeing and talking to them day in and day out. I also thank my parents, Dennis and Laura DiIorio, who have supported me throughout my life so that I could get to the point I am at at today.

## References

- [1] EJ Galvez, Charles H Holbrow, MJ Pysher, JW Martin, N Courtemanche, L Heilig, and J Spencer. Interference with correlated photons: Five quantum mechanics experiments for undergraduates. *American Journal of Physics*, 73(2):127–140, 2005.
- [2] HJ Kimble, M Dagenais, and L Mandel. Photon antibunching in resonance fluorescence. *Physical Review Letters*, 39(11):691–695, 1977.
- [3] Willis E Lamb Jr and Marlan O Scully. The photoelectric effect without photons. Technical report, DTIC Document, 1968.
- [4] R Hanbury Brown and RQ Twiss. A test of a new type of stellar interferometer on sirius. *Nature*, 178(4541):1046–1048, 1956.
- [5] Philippe Grangier, Gérard Roger, Alain Aspect, Antoine Heidmann, and Serge Reynaud. Observation of photon antibunching in phase-matched multiatom resonance fluorescence. *Physical Review Letters*, 57:687–690, 1986.
- [6] JJ Thorn, MS Neel, VW Donato, GS Bergreen, RE Davies, and M Beck. Observing the quantum behavior of light in an undergraduate laboratory. *American Journal of Physics*, 72:1210–1219, 2004.
- [7] Dietrich Dehlinger and MW Mitchell. Entangled photons, nonlocality, and bell inequalities in the undergraduate laboratory. *American Journal of Physics*, 70(9):903–910, 2002.
- [8] Mark Beck and Enrique Galvez. Quantum optics in the undergraduate teaching laboratory. In *Conference on Coherence and Quantum Optics*, page CSuA4. Optical Society of America, 2007.
- [9] Enrique J Galvez and Mark Beck. Quantum optics experiments with single photons for undergraduate laboratories. *Education and Training in Optics 2007*, 2007.
- [10] CH Holbrow, E Galvez, and ME Parks. Photon quantum mechanics and beam splitters. *American Journal of Physics*, 70(3):260–265, 2002.